HHS Public Access
Author manuscript
IEEE Trans Biomed Eng. Author manuscript; available in PMC 2020 April 01.

Published in final edited form as:
IEEE Trans Biomed Eng. 2019 April ; 66(4): 1148–1154. doi:10.1109/TBME.2018.2868830.

Acousto-optic Catheter Tracking Sensor for Interventional MRI Procedures

Yusuf Samet Yaras and **Sarp Satir [Member, IEEE]**
G.W. Woodruff School of Mechanical Engineering, Georgia Institute of Technology, Atlanta, GA, USA.

Cagla Ozsoy and **Ozgur Kocaturk**
Institute of Biomedical Engineering, Bogazici University, Istanbul, Turkey

Rajiv Ramasawmy, **Adrienne E. Campbell-Washburn**, and **Robert J. Lederman**
Division of Intramural Research, National Heart Lung and Blood Institute, National Institutes of Health, Bethesda, MD, USA.

F. Levent Degertekin [Senior Member, IEEE]
G.W. Woodruff School of Mechanical Engineering, Georgia Institute of Technology, Atlanta, GA, USA.

Abstract

Objective: The objective of this paper is to introduce an acousto-optic optical fiber sensor for tracking catheter position during interventional magnetic resonance imaging (MRI) to overcome RF induced heating of active markers.

Methods: The sensor uses a miniature coil coupled to a piezoelectric transducer, which is in turn mechanically connected to an optical fiber. The piezoelectric transducer converts the RF signal to acoustic waves in the optical fiber over a region including a fiber Bragg grating (FBG). The elastic waves in the fiber modulates the FBG geometry and hence the reflected light in the optical fiber. Since the coil is much smaller than the RF wavelength and the signal is transmitted on the dielectric optical fiber, the sensor effectively reduces RF induced heating risk. Proof of concept prototypes of the sensor are implemented using commercially available piezoelectric transducers and optical fibers with FBGs. The prototypes are characterized in a 1.5T MRI system in comparison with an active tracking marker.

Results: Acousto-optical sensor shows linear response with flip angle and it can be used to detect signals from multiple coils for potential orientation detection. It has been successfully used to detect the position of a tacking coil in phantom in an imaging experiment.

Conclusion: Acousto-optical sensing is demonstrated for tracking catheters during interventional MRI. Real-time operation of the sensor requires sensitivity improvements like using a narrow band FBG.

Significance: Acousto-optics provides a compact solution to sense RF signals in MRI with dielectric transmission lines.

Corresponding author: F. Levent Degertekin. levent.degertekin@me.gatech.edu.

Keywords

acousto-optic modulation; catheter; fiber Bragg grating (FBG); magnetic resonance imaging (MRI); optical fiber sensor; tracking

I. INTRODUCTION

Interventional device tracking and guidance in the body is essential for any interventional procedure. X-ray fluoroscopy is the leading medical imaging technology utilized for real time device-tracking purposes since X-ray fluoroscopy delivers high-resolution projection based images of metallic guidewires and tungsten or $BaSO_4$ doped catheters easily. However, there are intrinsic problems with X-ray fluoroscopy; it depicts soft tissue poorly and requires experienced eyes to determine the device position and orientation relative to anatomic landmarks.[1]. More importantly, medical staff and patient are exposed to harmful ionizing X-ray radiation during the entire procedure [2]-[5]. Magnetic resonance imaging (MRI) is an attractive imaging technology with several advantages for interventional procedures. MRI provides excellent soft tissue contrast; pathology and abnormalities can be detected at an earlier stage [6], [7]. Unlike other imaging techniques, different planes, standard or oblique, can be imaged without moving the patient. More importantly, MRI utilizes magnetic and electromagnetic fields, thus procedure is completely ionizing radiation free. Commercially available catheters compatible with X-ray fluoroscopy are mostly not MRI compatible or invisible under MRI due to the fundamental differences between MRI physics and X-ray physics. There are two main approaches, based on active and passive devices, to visualize devices under MRI [8]. Passive visualization relies on the material intrinsic magnetic properties. Ferromagnetic, paramagnetic and novel contrast agents can be utilized to enhance the visibility of catheters [9], [10]. Although passive visualization technique requires minimum device modification, it is still not a preferred technique for physicians due to obstruction of the surrounding anatomy and distortion in the MR images depending on the device orientation. Active visualization techniques requires incorporating RF receiver antennas [11], usually in small coil form, to collect localized RF signal [12]. While active catheter tacking systems offer conspicuity without obstructing the surrounding anatomy, they suffer from RF induced heating on the conductive transmission lines that transmit the RF signal out of body to MR scanner [13], [14]. Several methods such as detuning circuits [15], [16] and RF chokes [17], [18] were implemented to address RF induced heating. However, these techniques currently do not offer an active device design that can have clinically acceptable mechanical performance.

Dielectric transmission lines can be used instead of conducting electrical transmission lines to eliminate RF induced heating since dielectric materials do not absorb RF energy. As a dielectric transmission medium, optical fiber offers low insertion loss, mechanical flexibility, easy integration with electronics and immunity to RF heating. To use this method, a transduction scheme is needed to convert electrical signal to optical signal that will be guided within the optical fiber. Optoelectronic circuit based catheter tracking systems have been developed by several groups[19]-[22]; an optoelectronic circuit is used for electro-optic modulation where the circuit is powered by laser light carried via optical fiber. However, rigid and relatively large electronics and packaging used for the catheter tracking system makes this solution undesirable for practical interventional procedures. Another approach is using an intermediate coupling mechanism between electrical and optical domains, such as acousto-optic modulation. In acousto-optic modulation, elastic properties of optical medium are modulated using acoustic waves [23]. RF energy received by the antennas can be converted into acoustic waves by a piezoelectric transducer for acousto-optic modulation. One approach for such modulation scheme is interferometer based acousto-optic modulators utilizing reflectors and a reference beam [24]. Although interferometric transducers are easy to implement, they suffer from low sensitivity and mechanical stability. Another approach is employing Fiber Bragg grating (FBG). FBG based sensors have been widely employed for ultrasound detection for the past few decades [25]-[28]. FBG based acousto-optic modulators are small in size; gratings are already embedded in the dielectric transmission line, the optical fiber in this study, and the piezoelectric layers can directly be deposited over the optical fiber[29]. Moreover FBG modulators offer high bandwidth [30] and multiple FBGs can be easily fabricated on a single fiber [31] enabling multiple sensors on one optical fiber.

In this paper, we describe a sensor that relies on acousto-optic modulation technique for distal tip tracking of active catheters while eliminating RF induced heating risk due to the use of long conductor transmission lines. A preliminary version of this work has been reported [32]. The principle of operation for the proposed system is given in Fig. 1(a). RF signal is received by a small loop coil and used to drive a piezoelectric transducer. The piezo electric transducer is used to convert electrical signal to acoustic waves. Acoustic waves on a FBG sensor modulate the reflected light from the FBG sensor. Optical signal is carried out via optical fibers to a photo detector located away from MRI system. Electrical signal from the photo detector contains the spatial location information of the distal tip coil within the scanner. This paper is organized as follows: first, the operation principles of the sensor is given in Section 2; then, a proof of concept prototype is introduced in Section 3; experimental test results of the prototypes are given in Section 4; finally, several conclusions with a discussion of possible future performance improvements are provided in Section 5.

II. PRINCIPLE OF OPERATION

MRI is based on the nuclear magnetic resonance (NMR); hydrogen nuclei absorbs and emits electromagnetic radiation (RF signal) under magnetic field. Frequency of emitted RF field is proportional to the magnetic field, called Larmor frequency, governed by;

$$f_{RF} = \frac{\gamma}{2\pi}\left(B_0 + B_{gradient}\right) \quad (1)$$

where f_{RF} is the frequency of RF signal, γ is the gyromagnetic ratio, B_0 is the static magnetic field and $B_{gradient}$ is the gradient magnetic field used in order to distinguish different voxels from each other thus atoms in each voxel emit RF signal at a slightly different frequency.

RF receiver loop coils of active catheters receive signals from only nearby hydrogen nuclei of the surrounding anatomical location. The spatial location information is extracted from the RF signal transmitted to the scanner through conductive transmission lines. However, the conductor cables heat up during the interventional procedure due to the standing wave and eddy current formation [13].

The block diagram of the proposed catheter tracking sensor is shown in Fig. 1(a). Sensor system consists of four main components: a loop coil antenna to receive RF signal; a piezoelectric transducer to convert electrical signal to acoustic waves; an FBG sensor embedded in an optical fiber for acousto-optic modulation; and backend optoelectronics (light source and photodetector) for converting optical signal to electrical signal.

The loop coil antenna collects RF signal emitted by the nearby hydrogen atoms at frequency, f_{RF}. This time varying magnetic field going through a conductive loop induces a voltage due to Faraday's law of induction. Voltage induced on the coil is a function of time varying magnetic field and coil geometry; area and number of turns. A larger coil will produce more voltage whereas a smaller coil will provide more precise location information as the coil picks up RF signal from only the nearby atoms.

The piezoelectric transducer is connected to the terminals of receiver antenna, such that the induced voltage on the coil drives piezoelectric transducer. The vibration mode of the piezoelectric transducer and its geometry should be chosen such that the electrical input from the coil antenna is efficiently converted into acoustic waves in the FBG region of the optical fiber. In this particular case, a thickness mode piezoelectric transducer attached on a FBG sensor was used as thickness mode piezoelectric transducers that inherently have the highest electro-mechanical coupling and the thickness can be chosen so that a resonance of the transducer coincides with the Larmor frequency.

Fiber Bragg grating (FBG) is a type of distributed Bragg reflector; multiple mirrors in the fiber core are formed by periodic refractive index variations. FBG sensors have already been used as acousto-optic modulation sensors for nondestructive testing of structures [33]. Wavelength of the reflected light, called Bragg wavelength (λ_{Bragg}), strongly depends on the periodicity of the mirrors and refractive index of the fiber core [34]. FBG based acousto-optic modulation relies on the Bragg wavelength change by acoustic waves. Reflectivity spectrum of the FBG shifts due to both periodicity change of Bragg grating due to induced mechanical strain and refractive index change by elasto-optic effect. Fig. 1(b) illustrates the FBG based acousto-optic modulation technique used in this study. A narrow linewidth laser is used as input light source and wavelength of the laser is fixed on one of the side slope of notch in the FBG reflectivity spectrum. As the reflectivity spectrum of the FBG constantly shifts back and forth due to acoustic waves created by the piezoelectric transducer, power of the reflected light from the FBG is modulated since incoming light is fixed at a certain wavelength. A photo detector captures the reflected light from FBG sensor. Spectral information of the output signal from the photo detector gives the location information of the receiver coil. Note that the overall electrical length (a few millimeters) of conductive parts (coil antenna and electrodes of piezoelectric transducer) of a intravascular active catheter sample is much smaller than a quarter wavelength within the body (around 12 cm for 64

MHz) Therefore, RF induced heating risk is reduced significantly as compared to active sensors with conductive transmission lines.

III. Prototype Implementation

Proof of concept prototypes were built for an 1.5 Tesla interventional MRI system (Aera, Siemens Healthcare Systems) and tested in vitro. Using (1), f_{RF} is 63.87 MHz as the Larmor frequency at isocenter with a sensitivity of 85 kHz/meter for 20mT/meter gradient field. For a 1.2m long MRI bore, RF signal has a maximum bandwidth of 100 kHz.

The prototype consists of two main systems; an acousto-optic modulator probe and a back-end optoelectronic system for system control and MRI integration. overall system schematic is given in Fig. 2(a).

A. Acousto-optic probe

Acousto-optic probe incorporating a loop coil is placed at the catheter distal tip. It consists of a receiver coil for RF signal pickup, a piezoelectric transducer and a FBG sensor for acousto-optic modulation. Fig. 2(b) illustrates the acousto-optic probe designed for the prototype.

one of the primary design criteria for acousto-optic probe is size, mainly dictated by the coil. There is a trade-off between sensitivity and coil size as larger profile coils receive more RF signal emitted by the nearby atoms. The coil used in this prototype has a diameter of 3mm and length of 10mm with 40 turns offering small enough size for potential interventional applications. Note that the size of the coil can be further decreased with the expense of reduced signal.

Piezoelectric transducers have highest electro-mechanic coupling efficiency when operated at around their first resonance frequency [35]. Resonance frequency of thickness mode piezoelectric transducers is determined by their thickness, which is around 20–30 micrometer range for common piezoelectric materials for 63.87 MHz. Since it is difficult to fabricate and handle mechanically, a commercially available 100-μm thick piezoelectric transducer (Boston Piezo Optics Inc., MA, USA) with a resonance frequency of 21 MHz was used at its third harmonic resonance frequency of around 63 MHz. The measured electrical impedance of the particular piezoelectric transducer is shown in Fig. 3, which clearly shows the first and third harmonic mode resonances. Since the piezoelectric transducer is driven at its third harmonic, electromechanic coupling efficiency is significantly reduced.

Acoustic waves created by the piezoelectric transducer are coupled to FBG sensor via a rigid, Hertzian contact; FBG section of the fiber is attached to the piezoelectric transducer with low viscosity cyanoacrylate (3M Company, MN, USA). In order to increase sensitivity, a π phase shifted FBG was used in this study [36]. A phase shift, abrupt discontinuity on the grating, is introduced in the grating to create a Fabry-Perot cavity in the fiber with a very narrowband notch in the reflected wavelength spectrum, given in Fig. 1(b). Bragg wavelength is chosen as 1550 nm because of its extensive use in telecommunication. A commercially available π phase shifted FBG with 250 MHz central bandwidth (Teraxion Inc., Quebec, Canada) is used for acousto-optic modulation. The single mode optical fiber used at the distal end has a diameter of 250 μm with the acrylic protection layer. All components at the probe end are held together by a printed circuit board (PCB) piece for easy handling.

B. Back-end optoelectronic system

Back-end optoelectronic system handles the read-out from acousto-optic probe. Back-end optoelectronics schematic is given in the lower section of Fig. 2(b). A tunable laser source (NKT Photonics, Denmark) provides a narrow linewidth, less than 1 kHz, laser light. One way optical isolator is employed in order to prevent reflected light from FBG to go back into laser cavity. A three way optical coupler separates laser light going into the probe end and reflected light from probe end. Reflected light with its intensity modulated around the Larmor frequency from the FBG is captured by a high trans-impedance gain InGaAs photo detector with 125MHz bandwidth (New Focus Model 1811, CA, USA).

Gradient magnetic field change creates acoustic noise up to kHz due to Lorentz forces created on the gradient coils [37]. Since FBG sensor is sensitive to any elastic wave induced on the fiber, the acoustic noise also modulates the reflected light from the FBG. AC output from the photodetector is filtered with a band-pass filter to reject the AC signal caused by the acoustic noise. Filtered AC signal is analyzed with an oscilloscope. AC signal is also fed back into coil plug of MRI system, which is used for visualization of the active catheter.

Middle section of the side slope in the notch of FBG spectrum offers a linear operating region, Fig. 1(b). Therefore, it is crucial to ensure that laser wavelength is kept in the linear operating region of the FBG spectrum. Wavelength of the FBG can shift due to operating conditions such as temperature and mechanical load on FBG as well as high amplitude acoustic noise. Thus, a wavelength controller was designed based on an op-amp proportional-integral controller. The wavelength of the laser source is initially adjusted to desired point on the linear operating region of the FBG via temperature control on the laser source. DC output from the photodetector is used to track the power level of the reflected light from FBG. Dynamic changes in the FBG spectrum are tracked via piezoelectric wavelength adjustment in the laser source. Wavelength controller compares the DC output level with the set value and creates an error signal in the presence of a mismatch. Error signal is first amplified by a high voltage amplifier and then used for driving the piezoelectric actuator of the laser source. Wavelength controller can track wavelength changes up to 20 kHz, which covers all the acoustic noises frequencies. Note that, wavelength change created by mechanical loading and temperature changes on the FBG sensor has much lower frequency and are readily adjusted for by the controller.

C. Sensor operation with multiple coils

Position and orientation of the catheter tip are two parameters used for tracking purposes. Position information of distal tip can be obtained from single coil. However, at least two active markers are required in order to get the orientation information of the catheter tip,

[38]. Orientation information is especially important when catheter is guided through complex tortuous vasculatures.

In the proposed tracking sensor, one way to obtain multiple location information is incorporating multiple coils. A straightforward approach is to use multiple sensors on the same fiber since multiple FBG regions can easily be defined on single fiber. However this approach will make the back-end optoelectronics more complicated as each FBG requires individual laser sources and controller units. Another approach is to connect multiple coils at different locations on the catheter to a single acousto-optic modulator since the modulator has wide enough operation bandwidth and linear response at the low power levels generated by the coils.

In order to demonstrate multiple coil capability of the system, an experimental set-up is prepared as shown in Fig. 4 (a). Localized echo signals from the surrounding tissue inside the MRI system were emulated with large coils connected to a signal source. Large coils were air coupled to small coils of the probe. Two large coils are fed by the signal generator at the frequencies of 64 MHz and 64.001 MHz. 1 kHz frequency difference corresponds to a distance of 11.7 mm under 20mT/meter gradient field. Fig. 4(b) shows the frequency spectrum of the captured signal showing peaks at 64 MHz and 64.001MHz, indicating the feasibility of multiple coil readout.

Frequency response of the sensor is tested with the same experimental set-up but using only one coil. Frequency was swept between 63.8 MHz and 63.9 MHz covering the full frequency range of the aforementioned MRI system. Frequency response of the sensor is given in Fig. 4 (c). Mean of the amplitude is 82.8 mV with a standard deviation of 1.6 mV resulting in a relative standard deviation of 1.9% over 100 kHz.

IV. UNDER MRI TESTING RESULTS AND DISCUSSION

A prototype was tested in a water phantom model using a 1.5 Tesla MRI system (Aera, Siemens Healthcare Systems, Germany). The prototype was characterized before each experiment: first, the wavelength of the laser is swept in order to find the central notch of the FBG; then controller is set for 50% of the reflected power to ensure linear operation; finally, functionality of the probe is tested with a high amplitude RF pulse sequence in the MRI.

RF transmission signal, which is used to excite the atoms, was used for signal analysis and functionality tests, since RF transmission signal is much higher than the emitted RF signal by the atoms. The acousto-optic based sensor was compared with a conventional active marker; an identical coil connected to conducting transmission lines.

Fig. 5(a) shows the AC signal at the output of photodetector and conventional active marker for a spin-echo RF transmit signal. Acousto-optic sensor has a peak amplitude of 1.72 V whereas conventional marker has a peak amplitude of 50.7 V, which is 30 times higher than acousto-optic sensor. However, when the frequency spectrum is analyzed with normalized amplitudes, Fig. 5(b); there is only 10 dB difference between signal to noise ratios (SNR) for a bandwidth of 100 kHz; SNR of 57dB for the prototype and SNR of 67dB for the conventional active marker.

The prototype was further tested for linearity. Flip-angle is an important parameter to improve image contrast during MRI and it is directly proportional to the received RF signal amplitude. The prototype was tested for different flip angle values without changing any other MRI parameter. Fig. 6(a) compares the output signal from the acousto-optic sensor for flip angles of 20 and 40. The peak frequencies of both signals are exactly the same as the location of the sensor was not changed. The amplitude for 20° flip angle is 75 mV whereas 40° flip angle results in 148mV. The prototype sensor response was recorded for different flip angles ranging from 2° to 90°, shown in Fig. 6(b). Flip angle vs sensor signal amplitude is linear with a slope of 3.7mV/°, except for the region where flip angle approaches to 90° and the amplitude of the sensor saturates the photodetector. This can be prevented by reducing the laser power. In practice, small flip angle operation is favorable since higher flip angle sequences requires more time and elevates SAR values. When the sensor is used for tracking purposes with faster imaging sequences utilizing small flip angles, weak echo signal will not saturate the system.

Finally, another prototype sensor was tested and compared to an active marker for visibility in the MRI setting. A Gradient Echo (GRE) sequence with following parameters was used: Flip Angle, 90°:TR, 150 ms; TE, 3.4 ms for acousto-optic marker and Flip Angle, 15°; TR, 150ms; TE, 3.4 ms for active marker. Acquired MR images can be seen in Figure 7. In order to increase the visibility of acousto-optic sensor, an averaging of 32 was used. Locations of acousto-optic sensor and active marker are slightly shifted as both sensors and their corresponding coils were placed in same phantom side by side. MR image of acousto-optic sensor has a lower contrast compared to MR image of active marker due to lower amplitude and SNR.

Detection of the acousto-optic sensor position in the MR image is encouraging for further investigation of the proposed sensor scheme with improved sensitivity. Sensitivity can be improved with several straightforward ways. The sensitivity of the sensor is directly proportional to the slope of the FBG reflectivity curve (Fig. 1-b), which in turn is inversely proportional to the bandwidth of the FBG. By Using a readily available 50MHz bandwidth FBG [39] will improve the SNR by about 14dB. In the prototype, only a small portion of the power from the piezoelectric transducer is coupled to the FBG since lateral fiber dimension (125 μm in diameter) is much smaller than the lateral transducer dimension (1 mm). A custom thin film piezoelectric transducer coated over the optical fiber with overall resonance frequency tuned at Larmor frequency will increase the overall electro-mechanical coupling efficiency significantly by focusing the available power to the core of the optical fiber [40, 41]. Moreover, using a thin film coating approach will reduce the size of the sensor which is crucial for interventional procedures. These approaches to improve the sensor SNR beyond the corresponding active markers are currently being investigated.

V. CONCLUSION

An acousto-optic catheter tracking sensor for interventional MRI procedures has been presented. Prototype sensors were built by combining miniature receiver coils, commercially available piezoelectric transducers and optical fibers with integrated fiber Bragg grating for testing in 1.5T MRI systems. The sensor is shown to have a linear response with respect to

RF signal amplitude (flip angle). It is tested with multiple coils to demonstrate the possibility of orientation detection. The position tracking capability is demonstrated in a phantom experiment in comparison with an active marker. Although the current prototypes of the acousto-optical sensor have lower SNR as compared to an active marker using the same size coil, these initial results are promising with potential significant improvements on the Bragg grating bandwidth and electromechanical coupling by custom designed piezoelectric transducers. This dielectric transmission line based approach to acquire RF data during MRI can be useful for tracking as well as RF safety assessment with minimal image distortion or RF heating.

ACKNOWLEDGEMENTS

Research reported in this publication was supported by National Institute of Biomedical Imaging and Bioengineering of the National Institutes of Health under award number 5R21EB019098. The content is solely the responsibility of the authors and does not necessarily represent the official views of the National Institutes of Health. The authors do not have any financial interest to disclose.

The authors would like to thank Dr. Anthony Faranesh for his help during MRI testing of the prototype.

This work was supported by the NIH Grant 5R21EB019098.

REFERENCES

[1]. Ma Y et al., “Real-time x-ray fluoroscopy-based catheter detection and tracking for cardiac electrophysiology interventions,” Med. Phys, vol. 40, no. 7, p. 71902, 2013.

[2]. Efstathopoulos EP et al., “Medical personnel and patient dosimetry during coronary angiography and intervention.,” Phys. Med. Biol, vol. 48, no. 18, pp. 3059–68, 2003. [PubMed: 14529210]

[3]. Renaud L, “A 5-y follow-up of the radiation exposure to in-room personnel during cardiac catheterization.,” Health Phys, vol. 62, no. 1, pp. 10–15, Jan. 1992. [PubMed: 1727405]

[4]. Smith I, Cameron J, Mengersen KL, and Rivers JT, “Evaluation of coronary angiographic projections to balance the clinical yield with the radiation risk,” Br. J. Radiol, vol. 85, no. 1017, pp. 722–728, 2012.

[5]. BEDETTI G, BOTTO N, ANDREASSI MG, TRAINO C, VANO E, and PICANO E, “Cumulative patient effective dose in cardiology,” Br. J. Radiol, vol. 81, no. 969, pp. 699–705, Sep. 2008. [PubMed: 18508874]

[6]. Moore P, “MRI-guided congenital cardiac catheterization and intervention: The future?,” Catheter. Cardiovasc. Interv, vol. 66, no. 1, pp. 1–8, 2005. [PubMed: 16106421]

[7]. Lederman RJ, “Cardiovascular Interventional MRI,” Circulation, vol. 112, no. 19, pp. 3009–3017, Nov. 2005. [PubMed: 16275886]

[8]. Duerk JL, Wong EY, and Lewin JS, “A brief review of hardware for catheter tracking in magnetic resonance imaging,” Magn. Reson. Mater. Physics, Biol. Med, vol. 13, no. 3, pp. 199–208, 2002.

[9]. Bakker CJ, Hoogeveen RM, Hurtak WF, van Vaals JJ, Viergever MA, and Mali WP, “MR-guided endovascular interventions: susceptibility-based catheter and near-real-time imaging technique.,” Radiology, vol. 202, no. 1, pp. 273–276, Jan. 1997. [PubMed: 8988223]

[10]. Ratnayaka K et al., “Real-time MRI-guided right heart catheterization in adults using passive catheters,” Eur. Heart J, vol. 34, no. 5, pp. 380–389, Feb. 2013. [PubMed: 22855740]

[11]. Dumoulin CL, Souza SP, and Darrow RD, “Real-time position monitoring of invasive devices using magnetic resonance,” Magn. Reson. Med, vol. 29, no. 3, pp. 411–415, 1993. [PubMed: 8450752]

[12]. Yildirim DK, Sonmez M, Lederman RJ, and Kocaturk O, “A novel active device fabrication method for interventional MRI procedure,” in IFMBE Proceedings, vol 62, 2017, pp. 122–128.

[13]. Nitz WR, Oppelt A, Renz W, Manke C, Lenhart M, and Link J, “On the heating of linear conductive structures as guide wires and catheters in interventional MRI,” J. Magn. Reson. Imaging, vol. 13, no. 1, pp. 105–114, 2001. [PubMed: 11169811]

[14]. Sonmez M et al., “MRI active guidewire with an embedded temperature probe and providing a distinct tip signal to enhance clinical safety,” J. Cardiovasc. Magn. Reson, vol. 14, no. 1, pp. 1–10, 2012. [PubMed: 22226320]

[15]. Wong EY, Zhang Q, Duerk JL, Lewin JS, and Wendt M, “An optical system for wireless detuning of parallel resonant circuits,” J. Magn. Reson. Imaging, vol. 12, no. 4, pp. 632–638, 2000. [PubMed: 11042647]

[16]. Weiss S et al., “In vivo safe catheter visualization and slice tracking using an optically detunable resonant marker,” Magn. Reson. Med, vol. 52, no. 4, pp. 860–868, 2004. [PubMed: 15389956]

[17]. Susil RC, Yeung CJ, Halperin HR, Lardo AC, and Atalar E, “Multifunctional interventional devices for MRI: A combined electrophysiology/MRI catheter,” Magn. Reson. Med, vol. 47, no. 3, pp. 594–600, 2002. [PubMed: 11870847]

[18]. Ladd ME and Quick HH, “Reduction of resonant RF heating in intravascular catheters using coaxial chokes,” Magn. Reson. Med, vol. 43, no. 4, pp. 615–619, 2000. [PubMed: 10748440]

[19]. Fandrey S, Weiss S, and Muller J, “Development of an Active Intravascular MR Device With an Optical Transmission System,” IEEE Trans. Med. Imaging, vol. 27, no. 12, pp. 1723–1727, 2008. [PubMed: 19033088]

[20]. Sarioglu B, Aktan O, Oncu A, Mutlu S, Dundar G, and Yalcinkaya AD, “An optically powered CMOS receiver system for intravascular magnetic resonance applications,” IEEE J. Emerg. Sel. Top. Circuits Syst, vol. 2, no. 4, pp. 683–691, 2012.

[21]. Memis OG, Eryaman Y, Aytur O, and Atalar E, “Miniaturized fiber-optic transmission system for MRI signals,” Magn. Reson. Med, vol. 59, no. 1, pp. 165–173, 2008. [PubMed: 18098294]

[22]. Anders J, Sangiorgio P, Deligianni X, Santini F, Scheffler K, and Boero G, “Integrated active tracking detector for MRI-guided interventions,” Magn. Reson. Med, vol. 67, no. 1, pp. 290–296, 2012. [PubMed: 22135242]

[23]. Korpel A, Acousto-optics, vol. 57 CRC Press, 1996.

[24]. Hunsperger RG, “Acousto-Optic Modulators BT - Integrated Optics: Theory and Technology,” Hunsperger RG, Ed. New York, NY: Springer New York, 2009, pp. 201–220.

[25]. Rosenthal A, Razansky D, and Ntziachristos V, “High-sensitivity compact ultrasonic detector based on a pi-phase-shifted fiber Bragg grating.,” Opt. Lett, vol. 36, no. 10, pp. 1833–1835, 2011. [PubMed: 21593906]

[26]. Betz DC, Thursby G, Culshaw B, and Staszewski WJ, “Acousto-ultrasonic sensing using fiber Bragg gratings,” Smart Mater. Struct, vol. 12, no. 3, pp. 122–128, 2003.

[27]. Wild G and Hinckley S, “Acousto-ultrasonic optical fiber sensors: Overview and state-of-the-art,” IEEE Sens. J, vol. 8, no. 7, pp. 1184–1193, 2008.

[28]. Takahashi N, Yoshimura K, Takahashi S, and Imamura K, “Development of an optical fiber hydrophone with fiber Bragg grating,” Ultrasonics, vol. 38, no. 1, pp. 581–585, 2000. [PubMed: 10829730]

[29]. Wuethrich CR, Muller C. a. P., Fox GR, and Limberger HG, “All-fibre acousto-optic modulator using ZnO piezoelectric actuators,” Sensors Actuators A Phys, vol. 66, no. 1–3, pp. 114–117, 1998.

[30]. Fomitchov P and Krishnaswamy S, “Response of a fiber Bragg grating ultrasonic sensor,” Opt. Eng, vol. 42, no. 4, pp. 956–963, 2003.

[31]. Kersey AD, Berkoff TA, and Morey WW, “Multiplexed fiber Bragg grating strain-sensor system with a fiber Fabry--Perot wavelength filter,” Opt. Lett, vol. 18, no. 16, pp. 1370–1372, Aug. 1993. [PubMed: 19823386]

[32]. Yaras YS et al., “Acousto-optic Based Active MRI Marker for Interventional MRI Devices,” in ISMRM, 2017.

[33]. Betz DC, Thursby G, Culshaw B, and Staszewski WJ, “Acousto-ultrasonic sensing using fiber Bragg gratings,” Smart Mater. Struct, vol. 12, no. 1, p. 122, 2003.

[34]. Erdogan T, “Fiber grating spectra,” J. Light. Technol, vol. 15, no. 8, pp. 1277–1294, 1997.

Author Manuscript
Author Manuscript
Author Manuscript

[35]. Kino GS, Acoustic waves: devices, imaging and analog signal processing, no. 43 KIN 1987.

[36]. LeBlanc M, Vohra ST, Tsai TE, and Friebele EJ, “Transverse load sensing by use of pi-phase-shifted fiber Bragg gratings,” Opt. Lett, vol. 24, no. 16, pp. 1091–1093, 1999. [PubMed: 18073949]

[37]. Counter SA, Olofsson A, Grahn HF, and Borg E, “MRI acoustic noise: Sound pressure and frequency analysis,” J. Magn. Reson. Imaging, vol. 7, no. 3, pp. 606–611, 1997. [PubMed: 9170052]

[38]. Zhang Q, Wendt M, Aschoff AJ, Zheng L, Lewin JS, and Duerk JL, “Active MR guidance of interventional devices with target-navigation,” Magn. Reson. Med, vol. 44, no. 1, pp. 56–65, 2000. [PubMed: 10893522]

[39]. Teraxion Inc., “Custom fiber Bragg grating filters,” Teraxion Inc., 2013 [Online]. Available: http://www.teraxion.com/images/stories/pdf/MKT-FTECH-CUS_201312-3.1.pdf [Accessed: March. 14, 2018].

[40]. Godil AA, Patterson DB, Heffner BL, Kino GS, and Khuri-Yakub BT, “All-fiber acoustooptic phase modulators using zinc oxide films on glass fiber,” J. Light. Technol, vol. 6, no. 10, pp. 1586–1590, 1988.

[41]. Roe MP, Wacogne B, and Pannell CN, “High-efficiency all-fiber phase modulator using an annular zinc oxide piezoelectric transducer,” IEEE Photonics Technol. Lett, vol. 8, no. 8, pp. 1026–1028, 1996.

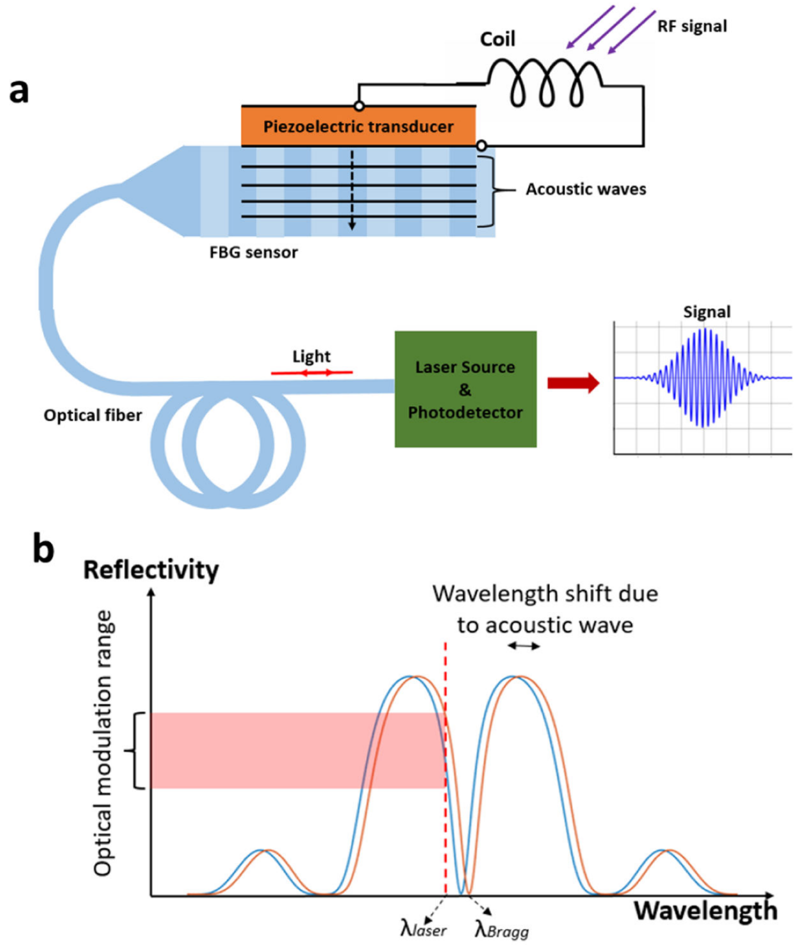

Figure 1.

(a) Block diagram of the FBG based acousto-optic catheter tracking sensor. Note that FBG sensor is embedded in the optical fiber, FBG part of the fiber is enlarged for illustrative purposes. (b) Acousto-optic modulation read-out scheme.

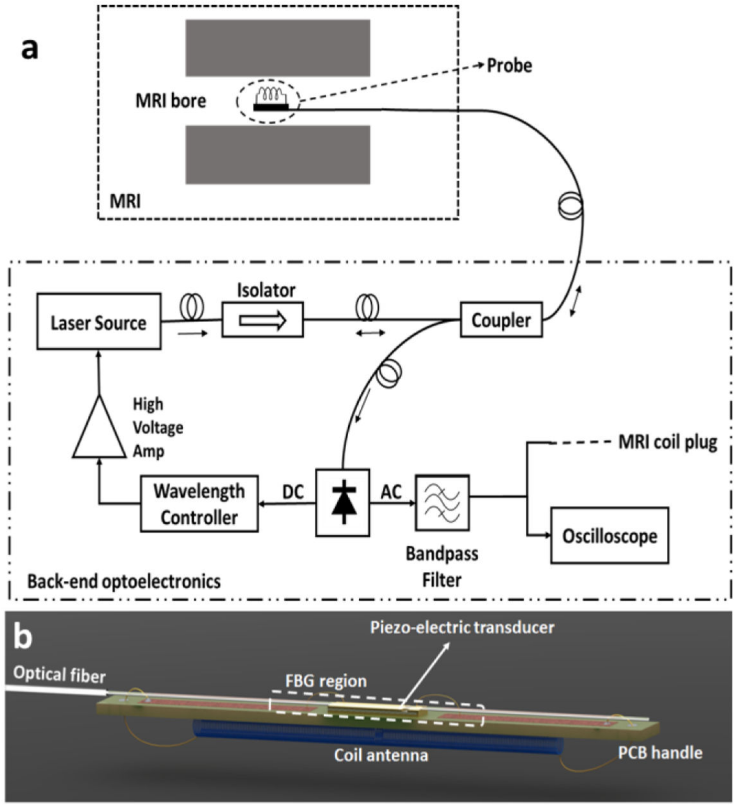

Figure 2.

(a) Schematic overview of the test setup. (b) Close up illustration of the acousto-optic probe showing receiver loop coil, piezoelectric transducer and FBG sensor.

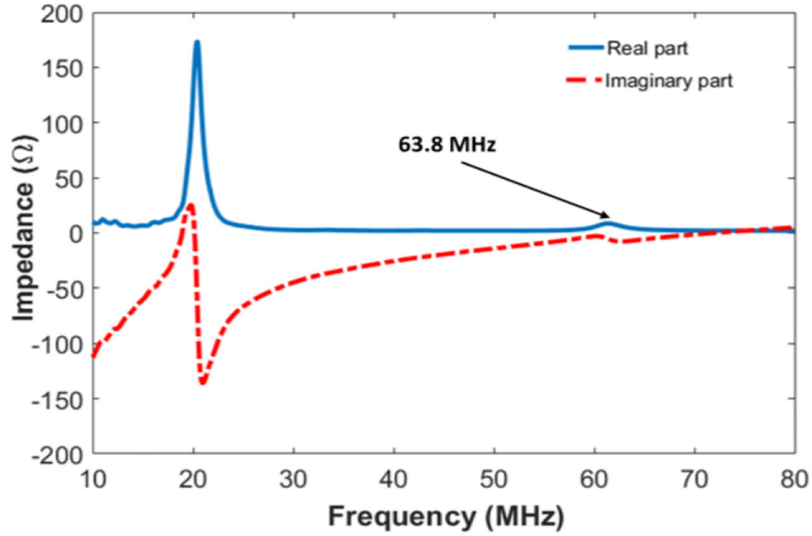

Figure 3.

Measured electrical input impedance of the piezoelectric transducer used to implement the sensor.

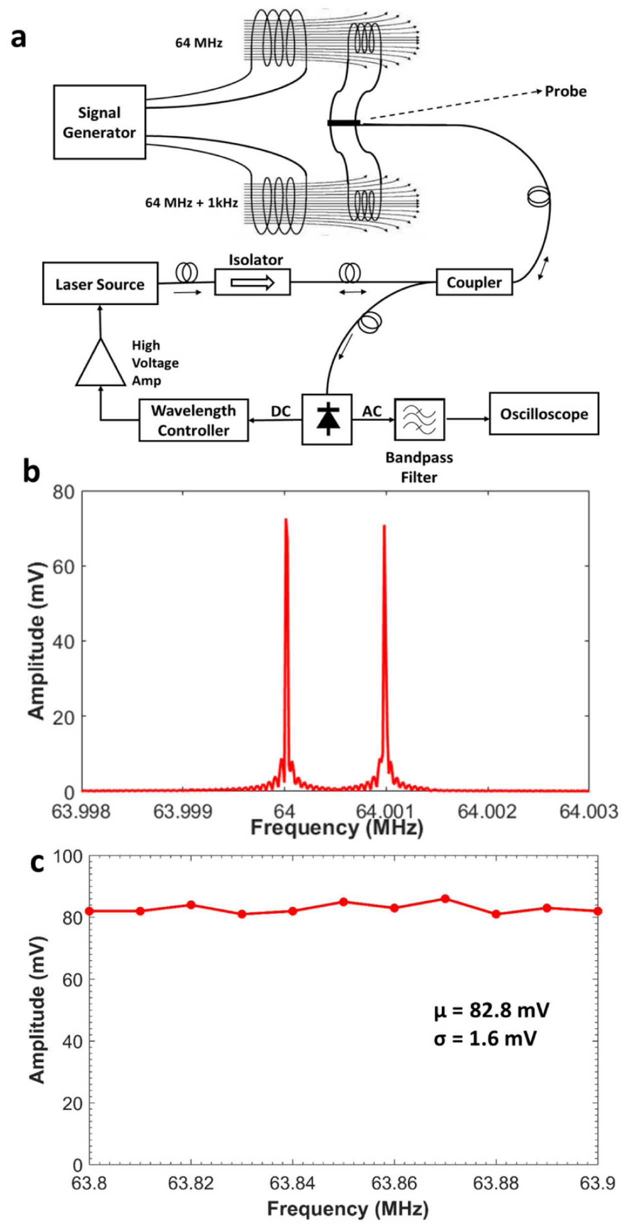

Figure 4.

(a) Experimental set-up for demonstration of multiple coil capability. (b) Frequency spectrum of the captured signal showing peaks at 64 MHz and 64.001 MHz. c) Frequency response of the sensor with single coil over 100 kHz range

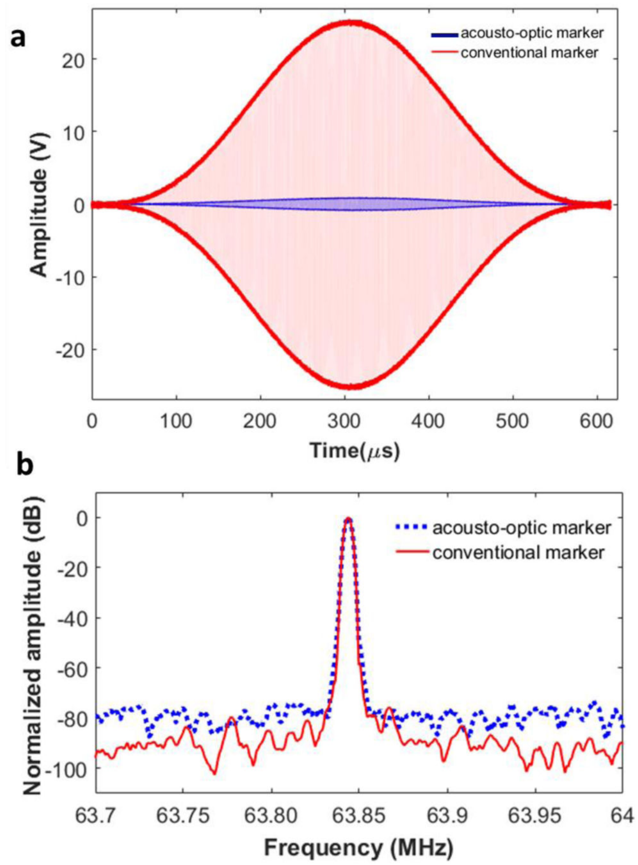

Figure 5.
(a) Comparison of acousto-optic sensor output and conventional marker for a spin-echo RF transmit signal (b) Normalized frequency spectrum of acousto-optic sensor and conventional marker for SNR comparison.

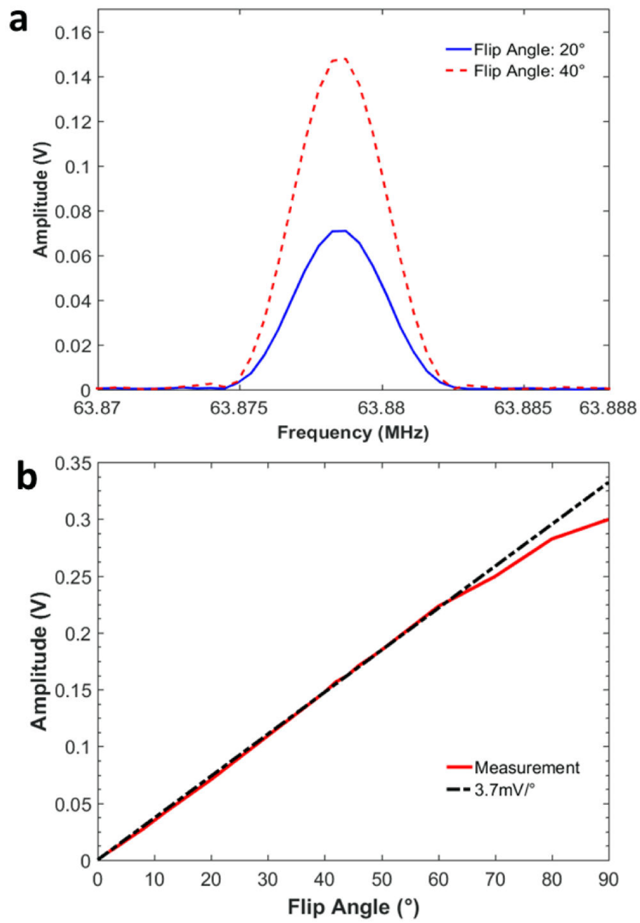

Figure 6.

(a) Acousto-optic sensor output for flip angles 20 and 40.(b) Acousto-optic sensor output vs flip angle

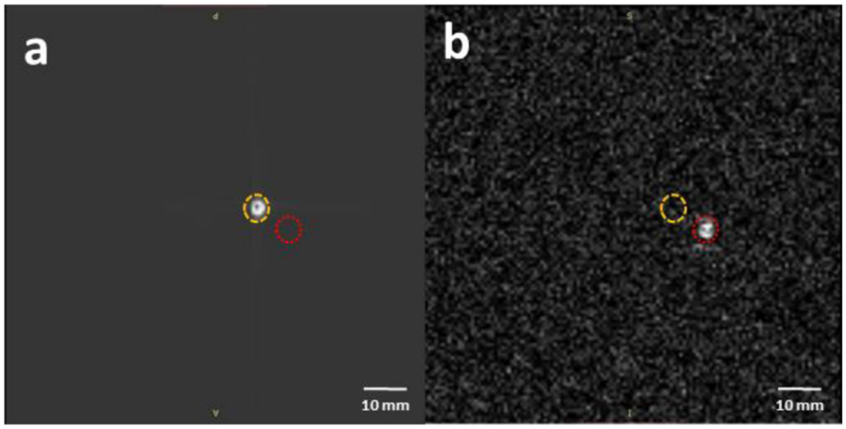

Figure 7.

MR image of (a) conventional marker, (b) acousto-optic marker using a GRE sequence and the device receiver channel only. Locations of acousto-optic marker and conventional cable connected marker are highlighted with red and yellow circles respectively